^{13}C-Labeled Platinum(IV)−Carbohydrate Complexes: Structure Determination Based on ^{1}H−^{1}H, ^{13}C−^{1}H, and ^{13}C−^{13}C Spin−Spin Coupling Constants

Henrik Junicke,[†] Anthony S. Serianni,*[,‡] and Dirk Steinborn*[,†]

Institut für Anorganische Chemie, Martin-Luther-Universität Halle-Wittenberg, Kurt-Mothes Strasse 2, D-06120 Halle/Saale, Germany, and Department of Chemistry and Biochemistry, University of Notre Dame, Notre Dame, Indiana 46556-5670

Received March 1, 2000

The reaction of D-mannose and D-allose with $[PtMe_3(Me_2CO)_3]BF_4$ **1** in acetone affords complexes $[PtMe_3L]BF_4$ **5** and **6** (**5**, L = α-D-mannofuranose; **6**, L = β-D-allofuranose). The coordination mode and conformation of the carbohydrate ligands in **5** and **6** in acetone-d_6 have been determined from an analysis of J_{HH}, J_{CH}, and J_{CC} in complexes formed using site-specific ^{13}C-labeled D-mannose and D-allose. These coupling data are compared to those measured in ^{13}C-labeled complex $[PtMe_3L]BF_4$ **2** (L = 1,2-*O*-isopropylidene-α-D-glucofuranose) and 1,2-*O*-isopropylidene-α-D-glucofuranose **3**, whose solid-state structures are known, and in ^{13}C-labeled 1,2;5,6-di-*O*-isopropylidene-α-D-glucofuranose **4**. The preferred furanose ring conformations in **2** and **5** are very similar (^{3}E/E$_4$ and E$_4$/^{o}E/E$_1$, respectively; eastern hemisphere of the pseudorotational itinerary), with platinum coordination involving O3, O5, and O6 of the saccharide. In contrast, the furanose ring of **6** prefers an ^{4}E/E$_o$/^{1}E geometry (western hemisphere of the pseudorotational itinerary) resulting from altered complexation involving O1, O5, and O6. Couplings within the exocyclic fragments of **2**, **5,** and **6** also support the existence of two different platinum coordination modes. In addition to establishing the structures and conformations of **2**, **5**, and **6** in solution, one-, two-, and three-bond J_{CH} and J_{CC} observed in these complexes provide new insights into the effect of structure and conformation on the magnitudes of these couplings in saccharides. Weak platinum(IV) complexation with the carbohydrate conformationally restricts the furanose and exocyclic fragment without introducing undesirable structural strain, thereby allowing more reliable correlations between structure and coupling magnitude.

Introduction

The complexation of carbohydrates with metals confers unique chemical and biological properties to this important class of biomolecules. For example, the complexation of molybdate with acyclic aldoses is highly selective and catalyzes C2-epimerization via a unique and stereospecific rearrangement of the carbon skeleton;[1a] a related reaction with 2-ketoses yields 2-*C*-(hydroxymethyl)aldoses via C2−C3 transposition.[1b] Similar remarkable arrangements are catalyzed by Ni(II).[1c] Metal ion (e.g., Mn(II), Co(II), Cd(II), Zn(II)) interactions with carbohydrates have been used to probe the specificities and mechanisms of enzyme-catalyzed reactions.[2,3] Given the abundance of potential ligands that can be displayed on saccharide skeletons having different relative configurations, and the range of metal ions present in the cell, it is possible that carbohydrate−metal complexes may be important in mediating presently unknown biological processes in vivo. Understanding the modes of metal binding to saccharides may also lead to the discovery of new chiral auxiliaries[4] for improved enantioselectivity in organic synthesis or to new metal−carbohydrate based pharmaceuticals.

We have been interested in reactions of transition metals with monosaccharides, with particular focus on platinum(IV). A new platinum reagent, $[PtMe_3(Me_2CO)_3]$-BF_4 **1**, was reported recently containing three acetone ligands that are readily displaced by specific arrangements of hydroxyl and other functional groups in saccharides in a manner that satisfies the octahedral coordination requirements of the platinum(IV) center.[5] The restricted ligation properties of **1** effectively eliminate the formation of oligomeric Pt(IV)−carbohydrate complexes that can complicate such studies, thereby allowing an evaluation of the types of monomeric carbohydrate complexes preferred by platinum(IV).

In a recent paper,[6] we prepared and characterized the Pt(IV)−carbohydrate complex **2** resulting from the reaction of **1** with 1,2-*O*-isopropylidene-α-D-glucofuranose **3** in acetone and established a ligation pattern involving O3, O5, and O6 of **3** (Scheme 1). The constitution of **2** was determined by mass spectrometry, X-ray crystallography, and NMR spectroscopy. NMR data were critical in establishing the solution structure of **2**, and in particular, the potential advantages of J_{CH} and J_{CC} values

* Authors for correspondence.
[†] Martin-Luther-Universität Halle-Wittenberg.
[‡] University of Notre Dame.

(1) (a) Hayes, M. L.; Pennings, N. J.; Serianni, A. S.; Barker, R. *J. Am. Chem. Soc.* **1982**, *104*, 6764−6769. (b) Hricoviniova-Bilikova, Z.; Hricovini, M.; Petrusova, M.; Serianni, A. S.; Petrus, L. *Carbohydr. Res.* **1999**, *319*, 38−46. (c) London, R. E. *J. Chem. Soc., Chem. Commun.* **1987**, 661−662.
(2) Sinnott, M. L. *Chem. Rev.* **1990**, *90*, 1171−1202.
(3) Bogumil, R.; Kappl, R.; Hüttermann, J.; Witzel, H. *Biochemistry* **1997**, *34*, 2345−2352.
(4) Piarulli, U.; Floriani, C. *Prog. Inorg. Chem.* **1997**, *45*, 393−429.
(5) Junicke, H.; Bruhn, C.; Ströhl, D.; Kluge, R.; Steinborn, D. *Inorg. Chem.* **1998**, *37*, 4603−4606.
(6) Junicke, H.; Bruhn, C.; Kluge, R.; Serianni A. S.; Steinborn. D. *J. Am. Chem. Soc.* **1999**, *121*, 6232−6241.

10.1021/jo000286q CCC: $19.00
Published on Web 06/01/2000

Scheme 1

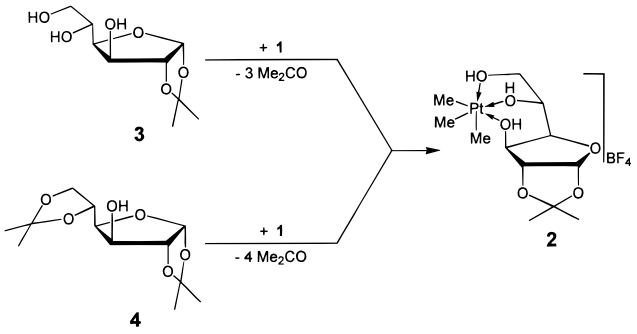

in the characterization were described. In this paper, we develop these scalar couplings more completely by interpreting the full complement of J_{CH} and J_{CC} values in site-specific ^{13}C-enriched **2**−**4**. Furthermore, the synthesis and structural characterization of two new complexes $[PtMe_3L]BF_4$ **5** and **6** (**5**, L = α-D-mannofuranose; **6**, L = β-D-allofuranose) are described containing site-specific ^{13}C-enrichment in the carbohydrate ligands. The results demonstrate that the D-mannose and D-allose ligands in **5** and **6** adopt the unexpected furanose form. In addition, due to the structural constraints imposed on the monosaccharide by metal complexation, NMR studies of **2**−**6** provide new insights into *J*-coupling behavior involving carbon in the furanose rings and exocyclic fragments of saccharides.

Experimental Section

Materials and General Procedures. D-[1-^{13}C]-, -[2-^{13}C]-, -[3-^{13}C]-, -[4-^{13}C]-, -[5-^{13}C]-, and -[6-^{13}C]glucose, D-[1-^{13}C]-, -[2-^{13}C]-, -[3-^{13}C]-, -[4-^{13}C]-, and -[6-^{13}C]mannose, and D-[2-^{13}C]-, -[3-^{13}C]-, and -[6-^{13}C]allose were provided by Omicron Biochemicals, Inc., South Bend, IN. Microanalyses were performed by the Microanalytical Laboratory in the Chemistry Department at Martin-Luther-Universität Halle-Wittenberg. $[(PtMe_3I)_4]$ was prepared as described previously.[7] All procedures were performed under anaerobic conditions using Schlenk techniques with purified argon. Acetone was dried over B_2O_3 and distilled under argon.

Synthesis of ^{13}C-Labeled 1,2-*O*-Isopropylidene-α-D-glucofuranoses. Singly ^{13}C-labeled D-glucoses (C1−C6) were converted to the corresponding ^{13}C-labeled 1,2;5,6-di-*O*-isopropylidene-α-D-glucofuranoses **4** according to literature procedures.[8] After recrystallization, the 5,6-*O*-isopropylidene group was removed selectively with sulfuric acid in water/methanol (1:1),[8] yielding ^{13}C-labeled 1,2-*O*-isopropylidene-α-D-glucofuranoses **3**.

Synthesis of $[PtMe_3(Me_2CO)_3]BF_4$ (1). $[(PtMe_3I)_4]$ (230 mg, 0.14 mmol) was added to a stirred solution of $AgBF_4$ (100 mg, 0.51 mmol) in acetone (20 mL) in the dark. After 30 min, AgI was removed by filtration, leaving a colorless solution that was used without further purification.

General Synthesis of $[PtMe_3L]BF_4$ Complexes. To a solution of **1** (270 mg, 0.51 mmol) in acetone (20 mL) was added with stirring a suspension of the carbohydrate L (0.54 mmol) in acetone (5 mL). After 12 h, the solvent was removed *in vacuo* and dried. The complexes were purified by one of two methods.

Method A. After being dissolved in methylene chloride (10 mL), the white $[PtMe_3L]BF_4$ precipitate was collected by filtration after 1 h, washed with a small amount of methylene chloride, and dried under argon.

Method B. The white $[PtMe_3L]BF_4$ precipitate was washed with methylene chloride (2 × 10 mL) and collected by filtration, washed with diethyl ether (2 mL), and dried under argon.

Synthesis of $[PtMe_3L]BF_4$ (2) (L = 1,2-*O*-Isopropylidene-α-D-glucofuranose). Workup: Method A. Yield: 116 mg (39%). Mp: 60 °C, dec above 145 °C (under argon). Anal. Calcd for $C_{12}H_{25}BF_4O_6Pt$: C, 26.34; H, 4.61. Found: C, 26.11; H, 4.93. ^{1}H NMR (500 MHz, −50 °C $(CD_3)_2CO$): δ = 1.03 (s + d, ^2J(Pt,H) = 78.8 Hz, 9H, PtCH_3), 6.83 (s, 3H, OH). ^{1}H NMR (500 MHz, $(CD_3)_2CO$): δ = 1.25 (s, 3H, CCH_3), 1.26 (s+d, br, ^2J(Pt,H), 9H, PtCH_3), 1.39 (s, 3H, CCH_3), 3.88 (dd, 1H, *H*6′, $^3J_{5,6'}$ = 5.9 Hz, $^2J_{6,6'}$ = 8.3 Hz), 3.95 (dd, 1H, *H*4, $^3J_{3,4}$ = 2.8 Hz, $^3J_{4,5}$ = 7.2 Hz), 4.10 (d, 1H, *H*3, $^3J_{3,4}$ = 2.8 Hz), 4.26 (ddd, 1H, *H*5, $^3J_{4,5}$ = 7.2 Hz, $^3J_{5,6}$ = 6.2 Hz, $^3J_{5,6'}$ = 5.9 Hz), 4.43 (d, 1H, *H*2, $^3J_{1,2}$ = 3.6 Hz), 5.84 (d, 1H, *H*1, $^3J_{1,2}$ = 3.6 Hz). ^{13}C{^{1}H} NMR (100 MHz; $(CD_3)_2CO$): δ = −11.58 (Pt(CH_3)$_3$), 26.4 (CH_3), 27.2 (CH_3), 67.6 (C6), 73.7 (C5), 75.2 (C3), 82.5 (C4), 86.6 (C2), 106.2 (C1), 112.7 ppm (O*C*O). ^{195}Pt{^{1}H} NMR (107 MHz; $(CD_3)_2CO$)): δ = 2350.

Synthesis of $[PtMe_3L]BF_4$ (5) (L = α-D-Mannofuranose). Workup: method B. Yield: 141 mg (51%). Mp 105 °C, dec above 134 °C (under argon). Anal. Calcd for $C_9H_{21}BF_4O_6Pt$: C, 21.32; H, 4.17. Found: C, 22.08; H, 4.58. ^{1}H NMR (500 MHz, −50 °C $(CD_3)_2CO$): δ = 1.03/1.09 (s + d, $^2J_{Pt,H}$ = 78.8 (6H) Hz/78.0 (3H) Hz, PtCH_3), 4.31 (s, 1H, O*H*2), 5.83 (d, 1H, O*H*1, $^3J_{1,OH}$ = 3.6 Hz), 6.60 (s, 2H, O*H*), 6.77 (s, 1H, O*H*); ^{1}H NMR (500 MHz, $(CD_3)_2CO$): δ = 1.16 (s + d, (br) $^2J_{Pt,H}$ = 79.1 Hz, 9H, PtCH_3), 3.86 (dd, 1H, *H*6′, $^3J_{5,6'}$ = 5.7 Hz, $^2J_{6,6'}$ = 8.4 Hz), 3.97 (dd, 1H, *H*6, $^3J_{5,6}$ = 6.6 Hz, $^2J_{6,6'}$ = 8.4 Hz), 4.07 (dd, 1H, *H*4, $^3J_{3,4}$ = 3.5, $^3J_{4,5}$ = 6.6 Hz), 4.28 (ddd, 1H, *H*5, $^3J_{4,5}$ = 6.6 Hz, $^3J_{5,6}$ = 6.4 Hz, $^3J_{5,6'}$ = 5.7 Hz), 4.52 (d, 1H, *H*2, $^3J_{2,3}$ = 6.0 Hz), 4.76 (dd, 1H, *H*3, $^3J_{2,3}$ = 5.9 Hz, $^3J_{3,4}$ = 3.5 Hz), 5.21 (s, 1H, *H*1). ^{13}C{^{1}H} NMR (150 MHz, $(CD_3)_2CO$): δ = −12.7 (s + d, $^1J_{Pt,C}$ = 781.3 Hz, PtCH_3), 67.1 (*C*6), 73.9 (*C*5), 80.6 (*C*3), 80.8 (*C*4), 86.7 (*C*2), 101.9 (*C*1). ^{195}Pt{^{1}H} NMR (107 MHz, $(CD_3)_2CO$): δ = 2541.

Synthesis of $[PtMe_3L]BF_4$ (6) (L = β-D-Allofuranose). Workup: method B. Yield: 156 mg (56%). Mp: 112 °C dec above 142 °C (under argon). Anal. Calcd for $C_9H_{21}BF_4O_6Pt$: C, 21.32; H, 4.17. Found: C, 21.78; H, 4.46. ^{1}H NMR (500 MHz, −50 °C $(CD_3)_2CO$): δ = 1.02/1.08 (s + d, $^2J_{Pt,H}$ = 78.7 (6H) Hz/77.9 (3H) Hz, PtCH_3), 4.63 (s, 1H, O*H*2), 5.94 (d, 1H, O*H*1, $^3J_{1,OH}$ = 3.6 Hz), 6.55 (s, 2H, O*H*), 6.78 (s, 1H, O*H*); ^{1}H NMR (500 MHz, $(CD_3)_2CO$): δ = 1.20 (s + d, (br) $^2J_{Pt,H}$ = 78.1 Hz, 9H, PtCH_3), 3.80 (dd, 1H, *H*6′, $^3J_{5,6'}$ = 5.2 Hz, $^2J_{6,6'}$ = 8.5 Hz), 3.90 (d, 1H, *H*4, $^3J_{4,5}$ = 9.2 Hz, 4.00 (dd, 1H, *H*6, $^3J_{5,6}$ = 6.2, $^2J_{6,6'}$ = 8.5 Hz), 4.15 (ddd, 1H, *H*5, $^3J_{4,5}$ = 9.2 Hz, $^3J_{5,6}$ = 6.2 Hz, $^3J_{5,6'}$ = 5.2 Hz), 4.50 (d, 1H, *H*3, $^3J_{2,3}$ = 6.0 Hz), 4.70 (d, 1H, *H*3, $^3J_{2,3}$ = 5.9 Hz), 5.22 (d, 1H, *H*1, $^3J_{1,OH}$ = 4.1 Hz), 5.40 (d, 1H, O*H*1, $^3J_{1,OH}$ = 4.1 Hz); ^{13}C{^{1}H} NMR (150 MHz, $(CD_3)_2$-CO): δ = −12.0 (s + d, $^1J_{Pt,C}$ = 789.1 Hz, PtCH_3), 68.1 (*C*6), 77.9 (*C*5), 83.2 (*C*3), 87.8 (*C*4), 88.3 (*C*2), 103.9 (*C*1); ^{195}Pt{^{1}H} NMR (107 MHz, $(CD_3)_2CO$): δ = 2514.

NMR Spectroscopy and Molecular Mechanics (MM2) Calculations. NMR spectra were obtained on Varian UNITY Plus 600 and Varian VXR-500S spectrometers in the Lizzadro Magnetic Resonance Research Facility at the University of Notre Dame (Notre Dame, IN) and on UNITY 500 and Gemini 2000 spectrometers at Martin-Luther-Universität Halle-Wittenberg using solvent signals (^{1}H, ^{13}C) as internal references. ^{1}H (600 MHz) and ^{13}C (150 MHz) spectra of free and complexed sugars were obtained on 0.01 M solutions in acetone-d_6 at 27 °C using a Nalorac 3 mm microprobe to enhance spectral S/N ratios of the natural abundance carbon signals and facilitate the measurement of spin-coupling constants. Since the ^{1}H and ^{13}C NMR spectra contained sharp signals for both free and metal-bound forms, and since spectra were obtained at high digital resolution, reported couplings are accurate to ±0.1 Hz. MM2 calculations were performed using Chem 3D Version 4.0 (CambridgeSoft).[9]

Results and Discussion

Although D-mannose and D-allose are insoluble in acetone, they react with $[PtMe_3(Me_2CO)_3]BF_4$ **1** within

(7) Baldwin, J. C.; Kaska, W. C. *Inorg. Chem.* **1975**, *14*, 2020.
(8) Schmidt, O. T. *Methods Carbohydr. Chem.* **1963**, *2*, 318−325.
(9) *Chemoffice 4.0; Chem3D Ultra 4.0, Cambridgesoft*, Cambridge, MA, 1997.

Scheme 2

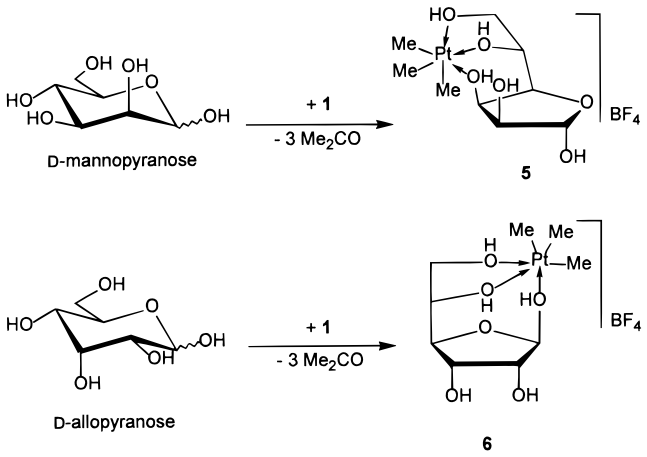

24 h to give $[PtMe_3L]BF_4$ **5** and **6** (**5**, L = α-D-mannofuranose; **6**, L = β-D-allofuranose) (Scheme 2). Under the same reaction conditions, D-glucose and D-galactose do not give complexes, but rather reduction to platinum metal occurs. The underlying cause for this difference in reactivity remains unclear.

The platinum−carbohydrate complexes were isolated as white, moisture-sensitive powders in good yields (**5**, 51%; **6**, 56%), and their identities were confirmed by microanalysis and by ^{1}H, ^{13}C, and ^{195}Pt NMR spectroscopy. The ^{195}Pt signals (**5**, 2541 ppm; **6**, 2514 ppm) of the complexes are observed at higher field than that of the tris(acetone) complex **1** (2696 ppm).[5] The following analysis will show that D-mannose and D-allose coordinate to the metal in their furanose forms through the two exocyclic hydroxyl groups at C5 and C6 and the hydroxyl group at C3 (**5**) and at C1 (**6**), respectively. This result is apparently caused by the preference of the *fac*-trimethylplatin(IV) moiety for facial binding tridentate carbohydrate ligands. Obviously, D-mannose and D-allose are not good tridentate ligands in their pyranose forms; both ligands convert into furanoses upon complexation with platinum(IV), through which sufficiently strong coordination with three hydroxyl groups is achieved. The furanoses revert rapidly to the more thermodynamically stable pyranoses upon addition of water to the platinum(IV)−carbohydrate complex, which cleaves the carbohydrate ligand and generates $[PtMe_3(H_2O)_3]BF_4$.

A. General Considerations. Compounds **2**−**6** contain two common structural elements: a furanose ring and an exocyclic CHOH−CH_2OH fragment. Conformational analysis of furanose rings is normally complicated by their inherent flexibility (pseudorotation), and consequently NMR spin-couplings within these rings are considered to be averaged in a fashion that reflects the presence of two or more interconverting forms in solution (Scheme 3). Exocyclic groups are also subject to conformational averaging in solution, imposing similar complications on the analysis of *J*-couplings within this fragment.

The presence of a 1,2-*O*-isopropylidene group in **2**−**4** introduces significant conformational constraints on furanose ring pseudorotation, and this effect can be exploited in the analysis of *J*-couplings sensitive to ring conformation. In addition, while the exocyclic moiety of **3**, and to a lesser extent that of **4**, is potentially flexible, this flexibility will be either highly reduced or eliminated in **2**. Consequently, *J*-couplings in the C5−C6 fragment of **2**, and of **5** and **6**, can be used to assist in the interpretation of related couplings in **3** and **4**. Likewise, *J*-couplings in the furanose rings of **2**, **5**, and **6** can be used to assist in the analysis of related values within the potentially more flexible furanose rings of **3** and **4**. This strategy will be applied to interpret J_{HH}, J_{CH}, and J_{CC} values in the following discussion. It should be appreciated that the structure of **2** was established with certainty previously,[6] so that its use in the analysis of spin-couplings in the new complexes **5** and **6** does not constitute a circular argument. In addition, we have found that, in general, the presence of platinum(IV) in the metal−carbohydrate complexes studied herein exerts little effect on J_{HH}, J_{CH}, and J_{CC} values within the saccharide, and thus, comparisons of corresponding couplings between free and complexed forms appear justified to a first approximation. This latter finding is not unexpected, since X-ray studies of complexes such as **2** reveal very long Pt−O bonds (∼2.2 Å), suggesting that coordination causes minimal perturbation or strain in the carbohydrate ligand. X-ray crystallography of **3**[10] shows that its furanose ring prefers a $^3T_4$ geometry (Scheme 3), and geometric optimization of this solid-state conformation using MM2[9] shifts this conformation slightly in favor of the E_4 form. This ring geometry also appears to be favored in aqueous and acetone solutions based on the very small $^3J_{H2,H3}$ (∼0 Hz), as suggested previously by Perlin and co-workers.[11a] Therefore, in the following discussion, we assume that the furanose ring of **3** prefers an $^3E/E_4$ geometry and interpret the remaining *J*-couplings in this context. MM2 optimization also leads to a preferred $^3E/E_4$ furanose ring conformation in **4**.

Scheme 3. Pseudorotational Itinerary of Aldofuranosyl Rings[a]

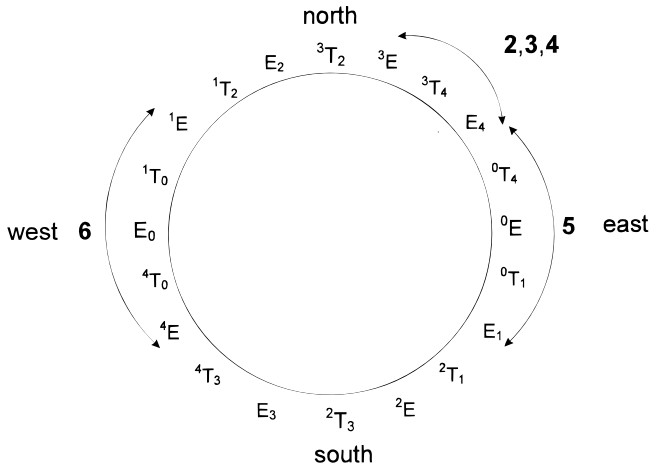

[a] E and T denote envelope and twist forms, respectively, and subscripts/superscripts denote the out-of-plane atoms.

(10) Takagi, S.; Jeffrey, G. A. *Acta Crystallogr., Sect. B* **1979**, *35*, 1522−1524.

(11) (a) Schwarcz, J. A.; Perlin, A. S. *Can. J. Chem.* **1972**, *50*, 3667−3676. (b) Tvaroska, I.; Hricovini, M.; Petrakova, E. *Carbohydr. Res.* **1989**, *189*, 359−362.

Scheme 4. Newman Projections of Staggered Rotamers in 3 about the C4−C5 Bond

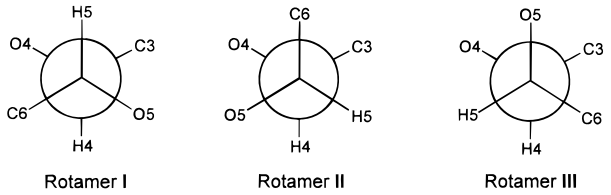

Scheme 5. Newman Projections of Staggered Rotamers in 3 about the C5−C6 Bond

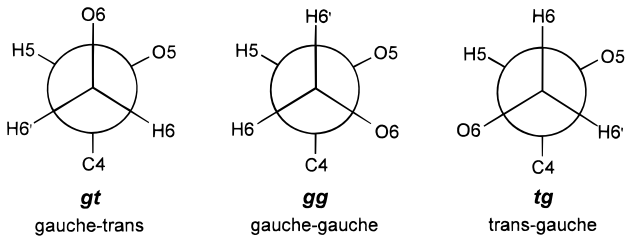

Table 1. $^3J_{HH}$ Values (in Hz) in 1,2-*O*-Isopropylidene-α-D-glucofuranose 3, 1,2;5,6-Di-*O*-isopropylidene-α-D-glucofuranose 4, and in the Platinum Complexes 2, 5, and 6 in Acetone

	compound					
coupled nuclei	**2**	**3**[a]	**3**	**4**	**5**	**6**
H1−H2	3.6	3.6	3.6	3.6	nc[b]	nc
H2−H3	nc	nc	nc	nc	5.9	6.0
H3−H4	2.8	2.7	2.7	2.7	3.5	1.0
H4−H5	7.2	9.4	7.5	7.2	6.5	9.2
H5−H6	6.3	2.7	3.5	6.2	6.4	6.3
H5−H6′	5.9	6.0	5.5	6.0	5.8	5.3
H6−H6′	−8.3	−12.1	−10.6	−8.4	−8.3	−8.5

[a] In ^2H_2O. [b] nc = no coupling (≤0.5 Hz).

C6) are observed. If the furanose ring of **3** prefers an $^3E/E_4$ conformation in aqueous solution, then Rotamer I is predicted to be more stable than Rotamers II and III based on assessments of the 1,3-interaction energies between O3 and substituents on C5. Rotamer I, however, does contain an unfavorable gauche effect (O4 and O5 are anti rather than gauche), which will be destabilizing relative to Rotamers I and III (Scheme 4). Potential intramolecular H-bonding between O3−H and O5−H is also possible in Rotamer I, possibly resulting in additional stability of this conformation in nonaqueous (acetone) solution. If Rotamer I is preferred in **3**, then the *tg* rotamer (Scheme 5) might be expected to be less stable than the remaining C5−C6 rotamers due to an unfavorable 1,3-interaction between O6 and the ring oxygen and to an unfavorable gauche effect (O5 and O6 are anti rather than gauche). These preliminary empirical considerations are taken as starting points in the analysis of *J*-couplings within the exocyclic fragment of **3**.

B. Spin-Couplings within the Furanose Rings. 1. Three-Bond $^1H-^1H$ Couplings. $^1H-^1H$ coupling constants within the furanose rings of 1,2-*O*-isopropylidene-α-D-glucofuranose **3** in water and acetone solvent, and of the platinum complex **2**, are nearly identical, indicating that ring conformation is highly conserved (Table 1). H1 and H2 are virtually eclipsed in **2** and **3**, but the measured $^3J_{H1,H2}$ of 3.6 Hz is significantly lower than expected (∼5.5 Hz) for the 18° torsion angle observed in the crystal structures of **2**[12] and **3**.[10] This result may be caused by the known reduction of $^3J_{HH}$ at anomeric carbons[13] and/or by the Barfield effect.[14] The latter effect is possible since the out-of-plane atom in the E_4 conformation lies opposite to the C1−C2 bond. Under these conditions, cisoidal $^1H-^1H$ couplings in furanose rings (e.g., $^3J_{H1,H2}$ in **2** and **3**) can be reduced by as much as 1 Hz; this effect has been substantiated in recent theoretical calculations of $^3J_{HH}$ in furanose models using density functional theory.[15] $^3J_{H2,H3}$ is essentially zero in **2**−**4**, indicating a H2−C2−C3−H3 torsion angle of ∼90°, according to a generalized Karplus curve;[16] in the crystal structure of **3**, the H2−C2−C3−H3 torsion angle is 82°. These couplings confirm the preferred ring conformation in **2** and **3** as $^3E/E_4$. The magnitude of $^3J_{H3,H4}$ (2.7−2.8 Hz) in **2**−**4** is smaller than expected (4.9 Hz) for a H3−C3−C4−H4 torsion angle of ∼50°; this result is probably due to the approximately trans orientation of O3 and H4 in the $E_4/^oE$ geometry, which is expected to reduce $^3J_{H3,H4}$.[17]

$^3J_{HH}$ values within the furanose ring of **5** suggest preferred furanose ring conformations near $E_4/^oE/E_1$ (Scheme 3). In these geometries, the H1−C1−C2−H2 torsion angle is ∼90°, which would yield a very small $^3J_{H1,H2}$. The small $^3J_{H1,H2}$ (≤0.5 Hz) also confirms the α-anomeric configuration of **5**; the *β*-configuration would yield a larger $^3J_{H1,H2}$ regardless of ring conformation. The large value of $^3J_{H2,H3}$ (5.9 Hz) is consistent with the near eclipsed H2 and H3 in $E_4/^oE/E_1$ geometries, and the magnitude of $^3J_{H3,H4}$ (3.5 Hz) suggests the same conformational preference.

$^3J_{HH}$ values in **6** suggest a significantly different platinum coordination mode in this compound. In contrast to **2** and **5** where O3, O5, and O6 coordinate to the metal, in **6** the carbohydrate ligand is coordinated through O1, O5, and O6. This complexation mode results in a preferred furanose ring conformation near E_o ($^4E/E_o/^1E$) (Scheme 3) in which the H1−C1−C2−H2 torsion angle is ∼90°, yielding a small $^3J_{H1,H2}$ (≤0.5 Hz). H2 and H3 are nearly eclipsed, resulting in a $^3J_{H2,H3}$ (6.0 Hz) similar to that found in **5** (5.9 Hz). In $^4E/E_o/^1E$ conformations, the H3−C3−C4−H4 torsion angle is ∼90°, and thus $^3J_{H3,H4}$ is small (1.0 Hz). The latter coupling provides strong evidence that platinum complexation does not involve O3; in a complex similar to that found for **2** and **5**, the H3−C3−C4−H4 torsion angle would be >160° and a larger $^3J_{H3,H4}$ would be expected.

2. Three-Bond $^{13}C-^1H$ Couplings. $^3J_{CH}$ in carbohydrates (i.e., $^3J_{CCCH}$ and $^3J_{COCH}$) depend largely on the torsion angle between the terminal atoms and on the nature of the intervening atoms.[11a,b] Corresponding $^3J_{CH}$ are similar within the furanose rings of **2** and **3** (Table 2), suggesting similar ring conformations, in agreement with the above conclusions based on $^3J_{HH}$. $^3J_{C1,H3}$ (4.9 Hz) in **2** and **3** is consistent with a torsion angle of ∼150°, while the small or zero values of $^3J_{C1,H4}$ and $^3J_{C2,H4}$ suggest C1−O4−C4−H4 and C2−C3−C4−H4 torsion angles of ∼90°, again consistent with a preferred $^3E/E_4$

(12) Steinborn, D.; Junicke, H.; Bruhn, C. *Angew. Chem.* **1997**, *109*, 2803−2805; *Angew. Chem., Int. Ed. Engl.* **1997**, *36*, 2686−2688.
(13) Bock, K.; Thøgersen, H. *Ann. Rep. NMR Spectrosc.* **1982**, *13*, 1−47.
(14) Marshall, J. L.; Walter, S. R.; Barfield, M.; Marchand, A. P.; Marchand, N. W.; Segre, A. L. *Tetrahedron* **1976**, *32*, 537.
(15) Cloran, F.; Carmichael, I.; Serianni, A. S. Personal communication.
(16) Haasnoot, C. A. G.; DeLeeuw, F. A. A. M.; Altona, C. *Tetrahedron* **1980**, *36*, 2783−2792.
(17) Günther, H. *NMR Spectroscopy*; J. Wiley and Sons: New York, 1995; p 119.

Table 2. $^{n}J_{CH}$ Coupling Constants (in Hz) in 1,2-*O*-Isopropylidene-α-D-glucofuranose 3, 1,2;5,6-Di-*O*-isopropylidene-α-D-glucofuranose 4 and in the Platinum Complexes 2, 5, and 6 in Acetone[a]

		compound					
coupled nuclei	*n*	**2**	**3**[c]	**3**	**4**	**5**	**6**
C1−H1	1	182.5	185.8	182.1	182.6	172.8	
C1−H2	2	5.5	5.3	4.8	5.3	1.7	
C1−H3	3	4.9	5.1	4.9	4.9	1.9	
C1−H4	3	nc	nc	nc	nc	nc	
C2−H1	2	5.5	5.5	5.4	5.4	nc	nc
C2−H2	1	159.8	162.6	159.7	159.8	159.8	157.7
C2−H3	2	2.6	2.6	2.7	2.8	1.9	2.3
C2−H4	3	nc	nc	nc	nc	nc	2.3
C3−H1	3	1.7	1.5	1.6	1.7	2.9	2.9
C3−H2	2	−1.0[b]	nc	nc	nc	3.2	2.9
C3−H3	1	152.8	154.9	152.9	152.0	158.5	156.9
C3−H4	2	+3.4[b]	2.9	2.6	nd	3.5	4.7
C3−H5	3	2.0	2.7	3.1	2.1	2.0	3.3
C4−H1	3	5.3	3.6	5.3	5.2	7.3	
C4−H2	3	3.7	3.5	3.6	3.7	2.5	
C4−H3	2	3.5	3.4	3.8	nc	5.7	
C4−H4	1	143.2	145.3	145.1	144.7	146.4	
C4−H5	2	nc	4.1	nd	0.7	nc	
C4−H6	3	3.1	3.8	2.6	3.1	3.4	
C4−H6′	3	3.5	nc	2.3	3.4	3.5	
C5−H3	3	nc	nc	nc	nc		
C5−H4	2	3.7	2.6	3.2	nd		
C5−H5	1	151.1	150.7	145.1	151.1		
C5−H6	2	nc	nc	1.4	nc		
C5−H6′	2	2.3	3.0	2.9	2.2		
C6−H4	3	3.1	2.6	2.5	3.4	3.5	2.8
C6−H5	2	nc	1.1	1.4	nc	nc	nc
C6−H6	1	148.9	143.4	140.4	148.9	149.1	149.5
C6−H6′	1	152.2	141.9	141.1	149.2	149.5	148.0

[a] For empty fields, couplings were not measured. nc = no coupling (≤0.5 Hz). nd = not determined due to signal overlap. [b] Sign determined experimentally. [c] In $^{2}H_2O$.

Table 3. $^{n}J_{CC}$ Coupling Constants (in Hz) in 1,2-*O*-Isopropylidene-α-D-glucofuranose 3, 1,2;5,6-Di-*O*-isopropylidene-α-D-glucofuranose 4 and in the Platinum Complexes 2, 5, and 6 in Acetone[a]

		compound					
coupled nuclei	n	2	**3**[d]	3	4	5	6
C1−C2	1	33.7	33.8	33.8	33.8	48.2	
C1−C3	2+3	nc	nc	nc	nc	nc	
C1−C4	2+3	nc	nc	nc	nc	nc	
C1−C5	3	4.4	4.0	4.3	4.5	4.3	
C2−C3	1	43.0	42.6	43.6	43.0	31.1	30.2
C2−C4	2+3	1.7	1.5	1.5	1.7	1.2	1.2
C2−C5	3	1.5	1.6	1.5	1.5	1.2	0
C3−C4	1	38.3	38.6	36.8	38.1	34.5	39.8
C3−C5	2	0.8	1.3	1.5	1.0	1.3	2.4
C3−C6	3	1.7	2.5	2.0	1.8	1.5	3.5
C4−C5	1	48.3	46.9	46.1	48.8	48.2	
C4−C6	2	nc	0.8	1.5	nc	nc	0.7
C5−C6	1	34.4	40.6	40.6	34.3	34.3	34.5
C1−CMe[b]	3	1.1	0.8	1.0	1.0		
C2−C_{iMe} [c]	2+3	1.5	1.5	1.0	1.4		
C2−CMe[b]	3	0.5	0.8	0.8	0.9		
C3−C_{iMe} [c]	2+3	2.5	2.5	2.5	2.5		

[a] For empty fields, coupling were not measured. nc = no coupling (≤0.5 Hz). [b] As assigned by NOE and HETCOR, the equatorial methyl group that appears at lower field than the axial methyl group is the only one showing couplings to C1 and C2. [c] Quaternary carbon atom of the isopropylidene group. [d] In $^{2}H_2O$.

conformation. $^{3}J_{C3,H1}$ in **2** (1.7 Hz) corresponds to a C3−C2−C1−H1 torsion angle of ∼115° and may be enhanced by the orientational effect of electronegative substituents[18] (i.e., the approximate trans disposition of O1 and C3 is expected to enhance $^{3}J_{C3,H1}$). $^{3}J_{C4,H1}$ in **2** and **3** in acetone are identical (5.3 Hz) and are consistent with a C4−O4−C1−H1 torsion angle of ∼140°.

$^{3}J_{C1,H3}$ in **5** is 1.9 Hz, indicating a reduced C1−C2−C3−H3 torsion angle relative to that in **2** and **3**, although the difference in the configuration at C2 may be partly responsible for the decrease (e.g., $^{3}J_{C1,H3}$ is small and 0 Hz in methyl α-D-glucopyranoside and methyl α-D-mannopyranoside,[18] respectively, despite nearly identical C1−C2−C3−H3 torsion angles). Like **2**, $^{3}J_{C1,H4}$ and $^{3}J_{C2,H4}$ remain small, indicative of C1−O4−C4−H4 and C2−C3−C4−H4 torsion angles of ∼100°. In contrast, $^{3}J_{C3,H1}$ is considerably larger in **5** (2.9 Hz) than in **2** (1.7 Hz), suggesting a larger C3−C2−C1−H1 torsion angle in the former (∼140°). $^{3}J_{C4,H1}$ is also larger in **5** (7.3 Hz) than in **2** (5.3 Hz), suggesting a larger C4−O4−C1−H1 torsion angle in the former. These data taken collectively suggest contributions from ^{o}E and E_1 conformers in solution for **5**, although the furanose rings of both **2** and **5** assume preferred geometries in the same general region of the pseudorotational itinerary (Scheme 3). This common ring geometry is assumed in **5** in the absence of conformational constraints imposed by a 1,2-*O*-isopropylidene ring; the quasiaxial or near-quasiaxial orientation of the C1−O1 bond in **5** may be critical to this observed behavior, since this orientation in furanose rings is favored over a quasiequatorial C1−O1 bond due to the anomeric effect.[19a−c]

In the preferred ring conformation of **6**, the C2−C3−C4−H4 torsion angle is ∼140°, compared to ∼90° in **2** and **5**, and $^{3}J_{C2,H4}$ is larger (2.3 Hz) in the former than in the latter (∼0 Hz). $^{3}J_{C3,H1}$ (2.9 Hz) is consistent with a torsion angle of ∼140°. A large coupling (7.3 Hz) is observed in **6** between C2 and O1-H, indicative of a ∼180° torsion angle between the coupled atoms. By comparison, $^{3}J_{C2,O3H}$ is 2.9 Hz in **2** and correlates with a 60° torsion angle between the coupled atoms.

3. Three-Bond ^{13}C−^{13}C Couplings. $^{3}J_{CC}$ values in carbohydrates depend on the C−C−C−C or C−O−C−C torsion angle and on the orientation of terminal and internal electronegative substituents with respect to the coupling pathway.[20−22] In the present investigation, complications arising from orientational effects of *internal* oxygens occur only for $^{3}J_{CCCC}$. A Karplus equation has been proposed for $^{3}J_{COCC}$, which takes torsional and terminal electronegative substituent effects into account, and there is evidence suggesting that the general characteristics of the $^{3}J_{CCCC}$ and $^{3}J_{COCC}$ Karplus curves are similar.[22]

The observed $^{3}J_{C1,C5}$ (4.3 Hz in acetone, 4.0 Hz in water) in **3** is larger than the expected coupling (3.2 Hz) for a C1−O4−C4−C5 torsion angle of ∼155° in $^{3}E/E_4$ conformations (Table 3). Conformation about the C4−C5 bond in **3**, however, will also affect $^{3}J_{C1,C5}$; one of these conformations (O5 anti to O4; Rotamer I, Scheme 4) is

(18) Podlasek, C. A.; Wu, J.; Stripe, W. A.; Bondo, P. B.; Serianni, A. S. *J. Am. Chem. Soc.* **1995**, *117*, 8635−8644.

(19) (a) Deslongchamps, P. *Stereoelectronic Effects in Organic Chemistry*; Pergamon Press Ltd.: Oxford, 1983. (b) Cossé-Barbi, A.; Dubois, J.-E. *J. Am. Chem. Soc.* **1987**, *109*, 1503−1511. (c) Serianni, A. S.; Barker, R. *J. Org. Chem.* **1984**, *49*, 3292−3300.

(20) Marshall, J. L. *Carbon−Carbon and Carbon-Proton NMR Couplings*: *Applications to Organic Stereochemistry and Conformational Analysis. Methods in Stereochemical Analysis*, Verlag Chemie International: Deerfield Beach, 1983; Vol. 2.

(21) Wray, V. *Prog. NMR Spectrosc.* **1979**, *13*, 177−256.

(22) Bose, B.; Zhao, S.; Stenutz, R.; Cloran, F.; Bondo, P. B.; Bondo, G.; Hertz, B.; Carmichael, I.; Serianni, A. S. *J. Am. Chem. Soc.* **1998**, *120*, 11158−11173.

Scheme 6

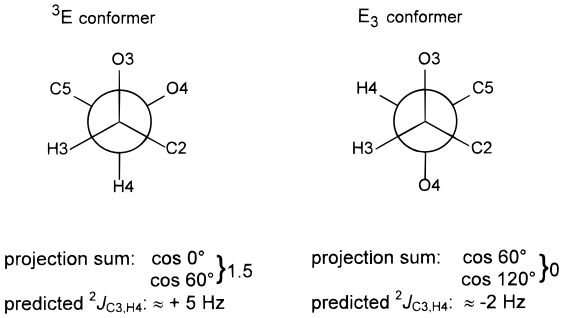

expected to enhance this coupling by ~0.6 Hz.[22] Although $^3J_{C1,C5}$ in **2** and **3** are similar, the in-plane effect[22] cannot occur in the former where Rotamer III (Scheme 4) is favored. The absence of the in-plane effect, however, is apparently offset by an increase in the C1−O4−C4−C5 torsion angle in **2** or by other factors. The C2−C3−C4−C5 torsion angle in $^3E/E_4$ conformations is also ~160°, but $^3J_{C2,C5}$ is 1.5 Hz in **2** and **3**. As indicated above, this coupling is influenced by internal and terminal electronegative substituents. For example, in *β*-D-gulopyranose where O3 and O4 are axial, $^3J_{C3,C6}$ is 1.8 Hz for a C3−C4−C5−C6 torsion angle of ~180°, whereas in *β*-D-glucopyranose where O3 and O4 are equatorial, $^3J_{C3,C6}$ = 4.4 Hz despite similar torsion angles.[22] The C3−C4−C5−C6 coupling pathway in *β*-D-gulopyranose mimics the C2−C3−C4−C5 coupling pathway in **2** and **3**, thus providing an explanation for the small $^3J_{C2,C5}$. The out-of-plane O5 (see below) will also further minimize the value of $^3J_{C2,C5}$ in **2**.

The similar preferred ring geometries in **2** ($^3E/E_4$) and **5** ($E_4/^oE/E_1$) result in similar values for $^3J_{C1,C5}$ (4.4 and 4.3 Hz, respectively) and $^3J_{C2,C5}$ (1.5 and 1.2 Hz, respectively). In contrast to the $^3J_{C2,C5}$ values in **2** and **5** which correlate with C2−C3−C4−C5 torsion angles of ~160°, $^3J_{C2,C5}$ in **6** is essentially zero, which is consistent with the reduced C2−C3−C4−C5 torsion angle expected in this complex (~100°). Importantly, since the C3−C4−C5−C6 torsion angle in **6** is nearly 0°, $^3J_{C3,C6}$ is considerably larger (3.5 Hz) than in **2** and **5** (~1.6 Hz) where the corresponding torsion angle is ~60° (estimated from the 63° torsion observed in the crystal structure of **2**).

4. Two-Bond $^{13}C-^1H$ Couplings. The magnitudes and signs of $^2J_{CCH}$ in carbohydrates can be predicted using a projection rule[23] that takes the relative orientation of electronegative substituents on both carbons in a C−C−H coupling pathway into account. $^2J_{CCH}$ values (Table 2) predicted using this method were found to be in qualitative agreement with observed couplings in the furanose rings of **2** and **3** if a $^3E/E_4$ geometry is assumed. Since $^2J_{CH}$ can be positive or negative in sign, 2D $^1H-^1H$ TOCSY data were collected on [3-^{13}C]**2** and cross-peak displacements used to establish the signs of $^2J_{C3,H4}$ and $^2J_{C3,H2}$;[24] the relative displacement observed for $^3J_{C3,H5}$ was used as the internal reference for a J_{CH} having positive sign. This sign information provides additional evidence of a preferred $^3E/E_4$ ring geometry in **2**. For example, significantly different couplings are predicted for $^2J_{C3,H4}$ in ^3E and E_3 conformations of **2** (Scheme 6). The observed values in **2** (+3.4 Hz) and **3** (+2.6 Hz, sign vide infra) (Table 2) are consistent with ^3E conformers. Similar observations are made for $^2J_{C4,H3}$; presumably the observed couplings in **2** (3.5 Hz) and **3** (3.8 Hz) are positive in sign.

The smaller $^2J_{C1,H2}$ in **5** (+1.7 Hz) relative to **2** (+5.5 Hz) results from the difference in configuration at C2. Projection sums for **2** and **5** are 1.5 and 1, respectively, and thus the observed couplings are expected to be positive, although the signs were not confirmed experimentally. $^2J_{C2,H1}$ is very small in **5** (≤0.5 Hz) but +5.5 Hz in **2**, again consistent with projection rule predictions (for **2**, ~+5 Hz; for **5**, ~0 Hz). The nearly eclipsed orientations of O2 and O3 in **5** lead to a projection sum of 1 for $^2J_{C2,H3}$ and a predicted coupling of ~2 Hz, in good agreement with the observed 1.9 Hz. $^2J_{C3,H2}$ is expected to be similar in magnitude to $^2J_{C2,H3}$ in **5**, but the former is larger (3.2 Hz). As expected, $^3J_{C3,H4}$ in **5** (3.5 Hz) is nearly identical to that found in **2** (3.4 Hz). In contrast, $^3J_{C4,H3}$ in **5** is 5.7 Hz, which is larger than that found in **2** (3.5 Hz). The latter difference may be partly due to remote effects on $^2J_{CH}$ values, which have been observed in aldopyranose rings.[18]

The difference in configuration at C1 in **6** compared to **2** results in a reduction in $^2J_{C2,H1}$ from +5.5 Hz to ~0 Hz, which is consistent with a change in projection sum from 1.5 (predicted $J \approx +5$ Hz) to 0.5 (predicted $J \approx 0$ Hz). Interestingly, despite the different C3 configurations in **2** and **6**, $^2J_{C2,H3}$ are similar (2.6 and 2.3 Hz, respectively). This observation is explained by the different preferred ring conformations in these complexes, which yield $^2J_{CH}$ values of nearly identical magnitude but of opposite sign (for **2**, projection sum: 0, predicted $J \approx -2$ Hz; for **6**, projection sum: 1.0, predicted $J \approx +2$ Hz). The projection sum of −0.5 derived for $^2J_{C3,H4}$ in **6** corresponds to a large negative coupling; the observed value (4.7 Hz) is consistent with expectations and is presumably negative in sign.

5. Dual-Pathway $^{13}C-^{13}C$ Couplings. Couplings between C1−C3, C1−C4, and C2−C4 in **2**−**6** (Table 3) are dual-pathway couplings (denoted $^{2+3}J_{CC}$) and are believed to be the algebraic sum of the couplings arising from both pathways.[25] If the latter assumption is valid, then an interpretation of $^{2+3}J_{C2,C4}$ is possible in **2** and **3**. The observed values are 1.5/1.7 Hz. If **2** and **3** contain furanose rings having conformations near $^3E/E_4$, then the C4−O4−C1−C2 torsion angle will be small (<15°). For this pathway, $^3J_{COCC}$ should be ~+3.0 Hz.[22] Thus, if the observed $^{2+3}J_{C2,C4}$ is equal to the algebraic sum of the couplings from both pathways, then $^2J_{C2,C4}$ must equal −1.4 or −4.6 Hz. The projection resultant[26] for $^2J_{C2,C4}$ equals zero, which corresponds to a predicted coupling of ~−2.0 Hz. By comparison, $^2J_{C3,C5}$ in methyl α-D-allopyranoside is 1.1 Hz,[18] and this coupling pathway, which is related structurally to the C2−C3−C4 pathway in **2** and **3**, also yields a projection resultant[26] of zero. Thus, the estimated value of −1.4 Hz for the two-bond contribution to $^{2+3}J_{C2,C4}$ in **2** and **3** appears reasonable, although sign determinations remain to be performed to validate this interpretation.

6. One-Bond $^{13}C-^{13}C$ Couplings. Theoretical studies of $^1J_{CC}$ in vicinal diol fragments suggest that coupling

(23) Bock, K.; Pedersen, C. *Acta Chem. Scand.* **1977**, *B31*, 354−358.
(24) Serianni, A. S., Podlasek, C. A. *Carbohydr. Res.* **1994**, *259*, 277−282.
(25) Bandyopadhyay, T.; Wu, J.; Stripe, W. A.; Carmichael, I.; Serianni, A. S. *J. Am. Chem. Soc.* **1997**, *119*, 1737−1744.
(26) Church, T.; Carmichael, I.; Serianni, A. S. *Carbohydr. Res.* **1996**, *280*, 177−186.

magnitude depends on the constituent C−C and C−O torsion angles.[27] These theoretical predictions have been confirmed recently in studies of carbohydrate−boron complexes.[28] Intra-ring $^1J_{CC}$ in **2**−**6** range from 30 to 49 Hz and can be divided into two groups. $^1J_{CC}$ between carbons bearing cis oxygens is 30−34 Hz, whereas $^1J_{CC}$ between carbons bearing trans oxygens is 43−48 Hz, and this dependence on O−C−C−O torsion angle is consistent with theoretical predictions.[27] For example, $^1J_{C1,C2}$ is larger in **5** (48.2 Hz) than in **2** (33.7 Hz), as expected since O1−O2 are trans in the former and cis in the latter, while $^1J_{C2,C3}$ is smaller in **5** (31.1 Hz) and **6** (30.2 Hz) than in **2** (43.0 Hz) since O1−O2 are cis in **5** and **6** and trans in **2**. In contrast, smaller differences of ∼5 Hz are observed between $^1J_{C3,C4}$ in **2** (38.3 Hz), **5** (34.5 Hz), and **6** (39.8 Hz); these couplings are of intermediate magnitude, presumably due to the intermediate O3−C3−C4−O4 torsion angle (∼90°).

7. One-Bond ^{13}C−^{1}H Couplings. In **2**−**6**, $^1J_{C1,H1}$ is significantly larger than the remaining intra-ring $^1J_{CH}$, and the presence of an isopropylidene group at C1 and C2 appears to further enhance this coupling. The magnitude of $^1J_{CH}$ in furanoses depends, in part, on C−H bond orientation (e.g., quasiaxial, quasiequatorial),[29a−c] although no clear trend can be discerned from the present data due to differences in ring conformation (e.g., **2** and **6**) and in the presence/absence of protecting groups (e.g., **2** and **5**). The latter factor could be significant, since such protection restricts C−O bond rotation and thus the disposition of oxygen lone-pairs with respect to nearby C−H bonds. The latter factor is known to influence C−H bond length, and thus presumably $^1J_{CH}$.[29a−c] It is worth noting that, in **2**, **3**, and **5**, $^1J_{C3,H3}$ is considerably larger than $^1J_{C4,H4}$. In the preferred $^3E/E_4$ ring conformation in these compounds, the C3−H3 bond is quasiequatorial and the C4−H4 bond is quasiaxial, and thus $^1J_{C3,H3}$ and $^1J_{C4,H4}$ are expected to be near their maximal and minimal values, respectively.

C. Spin-Couplings in the Exocyclic Fragments. 1. *J*-Couplings in the Exocyclic Fragment of 2, 5 and 6. Spin-couplings within the furanose rings of **2**, **5**, and **6** indicate identical metal coordination in **2** and **5** involving O3, O5, and O6, whereas metal coordination in **6** involves O1, O5, and O6. Involvement of the exocyclic C5−C6 fragment in platinum complexation is further supported by the magnitudes of $^1J_{C5,C6}$ in **2** (34.4 Hz), **5** (34.3 Hz), and **6** (34.5 Hz), which differ strongly from that observed in **3** (40.6 Hz), where rotation about the C5−C6 bond can occur. The smaller $^1J_{C5,C6}$ observed in the complexes is consistent with the reported effect of C−C torsion angle in vicinal diol fragments on $^1J_{CC}$;[27] $^1J_{CC}$ is considerably smaller when the two oxygens are cis than when they are trans. As a control, $^1J_{C5,C6}$ in **4** (34.3 Hz) is virtually identical to that observed in **2**, as expected since similar constraints are imposed on the C5−C6 torsion angle in both compounds.

Couplings between C3 and C6 of 1.7 and 1.5 Hz are observed in **2** and **5**, respectively, and are consistent with C3−C4−C5−C6 torsion angles of ∼60° found in their proposed structures. In contrast and as discussed above, $^3J_{C3,C6}$ is larger in **6** (3.5 Hz) and corresponds to the C3−C4−C5−C6 torsion angle of ≈ 0° found in its structure.

$^2J_{C4,C6}$ in **2** is small or zero. As reported previously,[6] the projection resultant for this coupling in the proposed structure of **2** is 1.5, which corresponds to a predicted zero coupling.[26] All other rotamers about the C4−C5 bond of **2** (and for **5** vide infra) yield projection resultants corresponding to predicted couplings of −2 Hz. The same approach extended to the proposed structure of **6** yields a projection resultant of 1.0, and the predicted small $^2J_{C4,C6}$ is consistent with experimental data (Table 3).

$^3J_{H4,H5}$ in **2** and **5** (7.2 and 6.5 Hz) are smaller than $^3J_{H4,H5}$ in **6** (9.2 Hz), indicating a reduction in the H4−C4−C5−H5 torsion angle from ∼40° (56° in the solid state) in **2** and **5** to ∼0° in **6**. The similar magnitudes of $^3J_{H5,H6}$ and $^3J_{H5,H6'}$ (6.3 and 5.9 Hz in **2**; 6.4 and 5.8 in **5**; 6.3 and 5.3 Hz in **6**) suggest that H5 is gauche to H6 and H6′ in all three complexes.

The torsion angle between C3 and H5 in **2** is 170° and is expected to be similar in **5**, but $^3J_{C3,H5}$ is only 2.0 Hz in both complexes (Table 2), a result that cannot be explained at present. The torsion angle between C3 and H5 in the proposed structure of **6** is ∼130°, which is consistent with the observed $^3J_{C3,H5}$ (3.3 Hz). $^3J_{C4,H6}$ and $^3J_{C4,H6'}$ are similar in **2** and **5** (3.1/3.5 Hz, and 3.4/3.5 Hz, respectively) and correlate with torsion angles of ∼40° for C4−H6 and ∼160° for C4−H6′ (49° and 167°, respectively, are observed in the crystal structure of **2**).

$^1J_{C5,H5}$, $^1J_{C6,H6}$, and $^1J_{C6,H6'}$ increase significantly upon platinum complexation; for example, these couplings are 145.1, 140.4, and 141.1 Hz in **3** (in acetone) and 151.1, 148.9, and 152.2 Hz in **2**, respectively. The origin of this effect is unknown, but may be caused by the five-membered ring involving O5 and O6, which causes an enhancement of $^1J_{CH}$ due to small bond length/angle changes in the C5−C6 fragment. A similar increase in the same $^1J_{CH}$ is observed in **4**, indicating that the metal is not responsible for the effect. In addition to the structural factors discussed above, this effect could be mediated by changes in the disposition of oxygen lone pairs on O5 and O6 with respect to the C−H bonds, which influences C−H bond lengths in carbohydrates and thus possibly $^1J_{CH}$ values.[29a−c]

2. *J*-Couplings in the Exocyclic Fragment of 3 and 4. $^3J_{H4,H5}$ is considerably larger for **3** in ^2H_2O solution (9.4 Hz) than in acetone solutions of **3** (7.5 Hz) and of **4** (7.2 Hz), suggesting a larger contribution from Rotamer I (Scheme 4). The larger $^3J_{C3,C6}$ observed in **3** (2.5 Hz) in ^2H_2O compared to **3** (2.0 Hz) and **4** (1.8 Hz) in acetone also supports this contention. However, $^3J_{H4,H5}$ values observed in **3** and **4** in acetone are very similar to $^3J_{H4,H5}$ observed in **2** (7.2 Hz) and **5** (6.5 Hz) where H4 and H5 are approximately gauche (Rotamer III, Scheme 4). Thus, Rotamer III cannot be excluded as a contributor to the C4−C5 rotamer population of **3** and **4** in acetone, although the small $^3J_{C3,H5}$ (2.1−3.1 Hz) appear more consistent with Rotamer I. $^2J_{C4,H5}$ is large in **3** in ^2H_2O solution (4.1 Hz), and it would be useful to establish its sign, since a negative sign is predicted for Rotamers I and III and a positive sign for Rotamer II. Thus, despite earlier claims that Rotamer I best describes C4−C5 bond conformation in **3**,[11a] the present coupling data do not yield an unequivocal assignment in **3** and **4**.

(27) Carmichael, I.; Chipman, D. M.; Podlasek, C. A.; Serianni, A. S. *J. Am. Chem. Soc.* **1993**, *115*, 10863−10866.

(28) Norrild, J. C.; Eggert, H. *J. Am. Chem. Soc.* **1995**, *117*, 1479−1484.

(29) (a) Serianni, A. S.; Wu, J.; Carmichael, I. *J. Am. Chem. Soc.* **1995**, *117*, 8645−8650. (b) Podlasek, C. A.; Stripe, W. A.; Carmichael, I.; Shang, M.; Basu, B.; Serianni, A. S. *J. Am. Chem. Soc.* **1996**, *118*, 1413−1425. (c) Church, T. J.; Carmichael, I.; Serianni, A. S. *J. Am. Chem. Soc.* **1997**, *119*, 8946−8964.

C5−C6 bond conformation in **3** in ^2H_2O and acetone appears to differ, as reflected in $^3J_{H5,H6}$ (2.7/3.5) and $^3J_{H5,H6'}$ (6.0/5.5) values. In **2**, the latter couplings are similar (6.3/5.9 Hz) and correlate with the *gg* rotamer (Scheme 5). In **2**, $^3J_{C4,H6/H6'}$ are ≈ 3.1/3.5 Hz. In contrast, these paired couplings differ significantly in **3** in ^2H_2O solution (3.8/≤0.5 Hz), and appear to favor the *tg* rotamer as do $^3J_{H5,H6/H6'}$ (Scheme 5). On the other hand, the *gt* rotamer appears more consistent with related coupling data in **4**.

D. $^{13}C-^{13}C$ Spin-Couplings Involving 1,2-*O*-Isopropylidene Carbons. Several $^3J_{COCC}$ values involving the methyl and quaternary (ipso) carbons of the 1,2-*O*-isopropylidene group were measured in **2**−**4**. C1 and C2 are coupled to only one of the methyl carbons, yielding values of 0.8−1.1 Hz for $^3J_{C1,CH_3}$ and 0.5−0.9 Hz for $^3J_{C2,CH_3}$; for $^3J_{C1,CH_3}$ and $^3J_{C2,CH_3}$, couplings to the same methyl group are observed (i.e., to the more downfield CH_3 signal that has been assigned by NOE and HETCOR as the equatorial methyl group). In contrast, coupling between C3 and the ipso carbon is 2.5 Hz in **2**−**4**. These couplings are interpreted in **3** for the purpose of illustration.

The crystal structure of **3** yields C1−CH_3 torsion angles of ∼97° and 138°, C2−CH_3 angles of ∼85° and ∼148°, and a C3−C(ipso) angle of 139°. MM2-optimized structures yielded corresponding values of ∼86° and ∼150°, ∼81° and ∼154°, and∼138°. We assume that these angles approximate those found in solution, taking conformational mobility into account. Thus, the $^3J_{C3,C(ipso)}$ value of 2.5 Hz corresponds to a torsion angle of ∼138°. A $^3J_{COCC}$ Karplus curve determined for carbohydrates[22] predicts a coupling of ∼2 Hz for this angle. The slightly larger observed value may be caused by the in-plane effect of O3 in the $^3E/E_4$ conformation, which has been shown to enhance these couplings by ∼0.6 Hz.[22]

Dihedral angles between C1 and C2 and the axial (more shielded) methyl carbon range from 81° to 97°, presumably accounting for the lack of coupling. In contrast, dihedral angles between C1 and C2 and the equatorial (more deshielded) methyl carbon range from 138° to 154°, and these pathways yield observed couplings of 0.5−1.1 Hz. The latter values are smaller than predicted from the $^3J_{COCC}$ Karplus curve.[22] The C2−O2−C(ipso)−CH_3(axial) pathway is similar to the C1−C2−O5−C6 coupling pathway in ketohexopyranoses, which exhibits smaller $^3J_{COCC}$ than the C1−O5−C5−C6 pathway in aldohexopyranoses on which the above-noted Karplus curve is based. The C1−O1−C(ipso)−CH_3(axial) pathway has not been studied previously, but its behavior is important to define since it mimics trans-*O*-glycosidic C−O−C−C pathways in structures such as α,α-trehalose.

Conclusions

This investigation has shown that an integrated analysis of J_{HH}, J_{CH}, and J_{CC} values in carbohydrate−platinum(IV) complexes leads to firm assignments of the metal coordination mode and conformation of the carbohydrate ligand. Measurements of J_{CH} and J_{CC} were facilitated by the use of singly ^{13}C-labeled carbohydrate ligands to simplify the coupling measurements, although uniformly ^{13}C-labeled ligands may also be employed to achieve the same end. More traditional approaches, which include coordination-induced shift (CIS) and linewidth analysis, are insufficient to establish the coordination mode and ligand conformation in these complexes, thus emphasizing the importance of the *J*-coupling approach exploited in this work.

J-coupling analysis has shown unambiguously that D-mannose and D-allose form complexes (**5**, **6**), upon reaction with **1**, in their α- and β-furanose forms, respectively. The latter forms are not favored in solution by either aldohexose, indicating that tautomeric equilibria can be shifted significantly upon metal complexation. Similar shifts in tautomeric equilibria have been observed in the formation of Ca^{2+} [30] and boronic acid[28] complexes with saccharides in aqueous solution. In both **5** and **6**, the exocyclic hydroxyl groups (O5-H, O6-H) are involved in platinum(IV) binding. The identity of the third ligand differs, being O3-H in **5** and O1-H (anomeric hydroxyl) in **6**. These different metal binding modes induce radically different furanose conformations in **5** and **6**, with the former preferring conformations near ^oE (east forms) and the latter preferring conformations near E_o (west forms) (Scheme 3).

In addition to the fundamental structural assignments obtained on these new carbohydrate-platinum(IV) complexes, useful new information on *J*-coupling behavior in saccharides evolved from this work. This information is summarized as follows:

(1) The large number of $^1J_{CC}$ values observed in **2**−**6** provides new experimental validation of theoretical predictions correlating $^1J_{CC}$ magnitude with C−C and C−O torsion angles in vicinal diol fragments.[27] These one-bond couplings appear particularly useful in identifying metal coordination sites involving vicinal diols in saccharides. By inference, other agents or bifunctional groups that complex these fragments in an analogous fashion might be expected to induce similar changes in $^1J_{CC}$ magnitude.

(2) Complex **6** provides the first example of a $^3J_{CCCC}$ value in a saccharide correlated with a C3−C4−C5−C6 dihedral angle (θ) of ∼0° (3.5 Hz). This coupling contrasts with the corresponding values in **2** and **5** (∼1.6 Hz), which are associated with torsion angles of ∼60°. These couplings complement $^3J_{CCCC}$ values obtained previously in aldohexopyranoses for $\theta = 180°$ (1.8−4.5 Hz depending on pathway configuration),[22,31] and are close in magnitude to $^3J_{COCC}$ for similar torsion angles,[22] providing evidence that $^3J_{COCC}$ and $^3J_{CCCC}$ do not differ appreciably in their dependence on torsion angle.

(3) The fixed furanose conformations in **2** and **3** ($^3E/E_4$) provide a reasonable system to interpret dual-pathway $^{2+3}J_{CC}$ within these rings. Although the uncertainties associated with the analysis are not negligible, the results suggest that $^{2+3}J_{CC}$ are approximated by the algebraic sum of their $^2J_{CC}$ and $^3J_{CC}$ components.

(4) The reaction of **1** with saccharides occurs without the loss of hydroxyl protons at the sites of complexation, and the structural constraints imposed by complexation *dictate the orientation of these protons*. Thus, in **6**, C2 exhibits a large coupling (7.3 Hz) to O1-H, whereas in **2**, C2 exhibits a coupling to O3-H of 2.9 Hz. These couplings represent limiting values for $^3J_{CCOH}$ in saccharides, the former for $\theta = 180°$ and the latter for $\theta = 60°$. These limiting values will provide useful tests of anticipated theoretical calculations of these couplings, whose Karplus

(30) Angyal, S. J. *Adv. Carbohydr. Chem. Biochem.* **1985**, *47*, 1−43.
(31) Wu, J.; Bondo, P. B.; Vuorinen, T.; Serianni, A. S. *J. Am. Chem. Soc.* **1992**, *114*, 3499−3505.

dependency is not well understood and whose potential as probes of C−O torsions (and hydrogen bonding) in saccharides has not been fully explored.

(5) In most cases, the use of projection rules[23,26] to interpret $^2J_{CH}$ and $^2J_{CC}$ values in **2**−**6** appears reliable, although some exceptions were observed. The latter suggest that other structural factors are at work (e.g., bond angle effects, effects of exocyclic C−O rotation) which are not adequately accounted for by the simple projection methods. In contrast, $^3J_{CH}$ and $^3J_{CC}$ appear to behave predictably based on known Karplus dependencies, suggesting that these couplings are less influenced by secondary factors.

The advantage of weak but specific complexation of platinum(IV) to saccharides provides a means to constrain the conformation of flexible structures such as furanoses without introducing undesirable structural strain in the molecule. Apart from their intrinsic value as novel compounds, these complexes hold promise as tools in the elucidation of *J*-coupling/structure correlations in carbohydrate systems. Logical extensions of this approach include platinum(IV) complexation with di- or oligosaccharides where *O*-glycoside linkage conformation might be constrained by specific metal binding, thereby providing a means to obtain trans-*O*-glycoside J_{CH} and J_{CC} values for defined linkage geometries.

Acknowledgment. The authors gratefully acknowledge financial support by the Deutsche Forschungsgemeinschaft and the Fonds der Chemischen Industrie and gifts of chemicals from Degussa (Hanau) and Merck (Darmstadt). The authors thank Omicron Biochemicals, Inc. (USA) for financial and technical support, and H.J. thanks Dr. Roland Stenutz for helpful discussions.

JO000286Q